UPPER OCEAN SALINITY STRATIFICATION AND RAIN FRESHENING IN THE TROPICS OBSERVED FROM AQUARIUS

Thomas Meissner, Frank Wentz, Joel Scott and Kyle Hilburn

Remote Sensing Systems, Santa Rosa, California, USA.

ABSTRACT

We present validation results for the Aquarius Version 3.0 ocean surface salinity product that has been released in June 2014. We focus on comparing the Aquarius salinity in the tropics with measurements from the ARGO drifter network, moored PMEL buoys and HYCOM. The results are stratified as function of surface rain rate. As the measurements occur at different depth below the ocean surface, this allows an assessment of salinity stratification within the very upper ocean layer and rain induced freshening effects. We separate the rain freshening effects from local biases in the Aquarius salinity that correlate with sea surface temperature and are likely related to uncertainties in the geophysical model that is used in the salinity retrieval algorithm. We derive an adjustment for this SST-dependent biases and evaluate the performance of this bias-adjusted salinity product. A comparison between the standard Aquarius salinity product and the CAP salinity is also presented.

Index Terms— Aquarius, Ocean Surface Salinity, Stratification.

1. BACKGROUND

The Aquarius L-band radiometer/scatterometer system is designed to provide monthly salinity maps at 150 km spatial scale at an accuracy of 0.2 psu [1].

Our study is based on the Aquarius Version 3.0 salinity product that has been released in June 2014. The details of this products and the algorithm that is used in its retrieval can are described in [5], [6], [7].

The CONAE Microwave Radiometer (MWR) supplies brightness temperatures at K/Ka-band that are exactly spatially and temporally collocated with the Aquarius salinity observations [2]. It is straightforward to adapt the UMORA rain retrieval algorithm [3] to retrieve rain rates from MWR. Together with the Aquarius salinity product, the MWR thus provides an invaluable tool for studying rain effects on ocean surface salinity [4].

2. AQUARIUS VERSUS ARGO SALINITY

Figure 1 shows the difference of monthly ocean surface salinity averages between Aquarius and the ARGO buoy network. All Aquarius observations have been filtered for rain using the MWR rain rate retrievals. The ARGO data are taken from the monthly 3-deg gridded ADPRC field provided by the University of Hawaii (apdrc.soest.hawaii.edu).

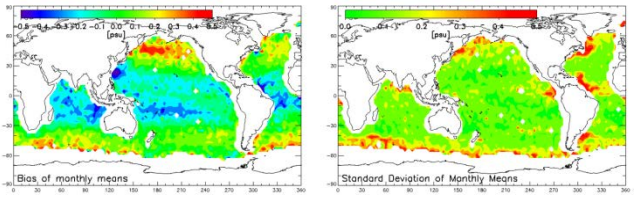

Figure 1: Bias (left) and standard deviation (right) between monthly 150 km means of ocean surface salinity from Aquarius after rain-filtering and ARGO.

In many locations over the open ocean the 0.2 psu accuracy requirement is met. However, significant salty biases in the Aquarius salinity when compared to ARGO are observed at mid-high latitudes, whereas fresh biases are observed throughout the tropics and subtropics. These large-scale biases dominate the Aquarius V3.0 SSS error budget. The fresh biases in the tropics occur even though the Aquarius events have been screened for rain.

3. DATA SETS

Ocean Surface Salinity				
Data Source	Aquarius V3.0 L2	ARGO (ADPRC)	HYCOM	PMEL moored buoys
Depth	few cm of surface	5 m	≈ 5 m	1 m
Temporal/spatial resolution and matching	100 – 150 km	3 deg monthly	1/12 deg daily	averaged within 150 km of AQ daily

Table I: Data sources for ocean surface salinity used in this study.

Rain Rate				
Data Source	MWR (CONAE)	WindSat	F17 SSMIS	TMI
Resolution	35 – 47 km	10 km	32 km	15 km
Time	instance of AQ	1 hour within AQ	1 hour within AQ	variable time

Table II: Data sources for surface rain rate used in this study.

Table I and Table II list the data sources for salinity and rain rate that are used in our study and their major properties. The various satellites used in obtaining the rain rates have

different equatorial crossing times relative to Aquarius. This allows looking at rain events that occur at different times relative to the Aquarius salinity measurement.

The time interval for our study is the 2-year period September 2011 – August 2013.

4. RAIN FRESHENING EFFECTS AND STRATIFICATION

Using our collocated SSS – rain rate data sets (section 3) we can assess both the size of rain freshening effect in the upper layer depending on rain intensity as well as the time scale during which mixing of the upper layer occurs (Figure 2).

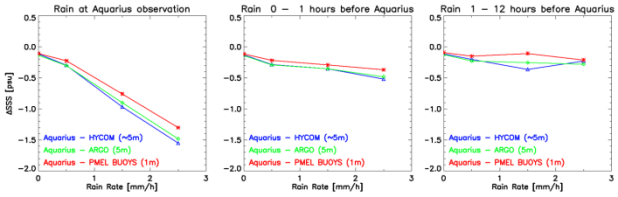

Figure 2: SSS difference between Aquarius and ARGO, PMEL buoys and HYCOM stratified by surface rain rate: Left panel = Rain at the Aquarius observation. Center panel = No rain at the Aquarius observation but within 1 hour before the Aquarius observation. Right panel: No rain at or up to 1 hour before the Aquarius observations, but rain 1 – 12 hour before the Aquarius observation.

	Aquarius - ARGO		Aquarius - HYCOM		Aquarius - PMEL	
	Standard	Bias adj.	Standard	Bias adj.	Standard	Bias adj.
No Rain	-0.14	+0.01	-0.11	+0.03	-0.11	+0.03
Rain	-0.36	-0.18	-0.35	-0.18	-0.27	-0.10
Total	-0.18	-0.03	-0.16	-0.01	-0.14	+0.01

Table III: Salinity biases between Aquarius and ARGO, HYCOM, PMEL at the location of the PMEL buoys. The values are given for cases without any rain, with rain and for all cases. The left columns show the results for the standard Aquarius V3.0 salinity product. The right columns show the results after the SST dependent bias adjustment (section 5).

In the left panel of Figure 2 rain is occurring at the instance and location of Aquarius. A strong freshening of the Aquarius salinity when compared to the other measurements is evident. Most of this freshening is due to rain dilution in the surface layer [4], though at low wind speeds rain splashing effects might also play a role [8]. In the center panel there is no rain at the Aquarius observation but rain occurs within 1 hour before. There is a clear freshening effect visible that correlates with rain rate. The freshening is slightly larger when compared to the 5 m depth measurements (ARGO, HYCOM) than when compared to the 1 m depth measurement (PMEL). The only explanation for this observation is a freshwater lensing effect that does not mix within the 1 hour between rain and the Aquarius measurement. When the time window is increased to 1 -12 hours (right panel), the freshening effect and its correlation with rain rate has ceased. So we can conclude that on average the upper ocean layer between surface and 5 m depth has mixed.

Table III lists the total biases between Aquarius and the various other measurements at the location of the tropical PMEL array separated in cases without and with rain. The values are in good qualitative and quantitative agreement with the results from SMOS [4].

5. SST DEPENDENT SALINITY BIASES

5.1 Causes of SST Dependent Biases

All of our results presented so far indicate that the Aquarius V3.0 salinity exhibits fresh biases in the tropics and salty biases at mid-high latitudes, which are not related to rain freshening or stratification. These biases correlate with sea surface temperature and are likely caused by small, residual errors in the geophysical model function that is used in the SSS retrieval algorithm. The most probable candidates are:

1. Uncertainties in the dielectric constant model [9], [10]. A comparison of surface emissivities from various dielectric models at L-band shows that the brightness temperature differences between these models are as large as the brightness temperature differences that would be caused by the observed SSS biases.

2. Uncertainties in the oxygen absorption at L-band. L-band lies in the O_2 continuum and is far from the O_2 resonance lines at 50 – 60 GHz, which makes the L-band atmospheric absorption model prone to uncertainties [11].

Another possible source for SST dependent biases is the surface roughness correction: For example, the SST dependence of the wind induced emissivity that has been assumed in [6] and [10] is likely only approximately valid.

5.2 Bias Adjustment

Most likely one is dealing with a combination of some or all of these error sources. The magnitude of the observed SSS biases translates into a radiometric error of the order of 0.2 Kelvin. On that level it is very difficult to disentangle the various contributions in the geophysical model function and adjust them individually. It is therefore warranted to make a simple SST dependent post-hoc adjustment ΔSSS_{bias_adj} to the retrieved SSS in order to mitigate the observed biases [5]. The form of this adjustment is displayed in Figure 3. In order to derive this curve the bias between Aquarius and HYCOM salinity has been regressed to SST. The values displayed in Figure 3 are subtracted from the standard Aquarius V3.0 salinity product. The same adjustment is used for all three Aquarius horns. Its form is:

$$\Delta SSS_{bias\_adj}(T_S) = -0.0019594 \cdot T_S^{\,2} + 1.1257 \cdot T_S - 161.4934$$

where the units are Kelvin for T_S and psu for ΔSSS .

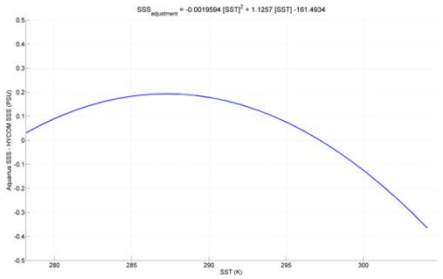

Figure 3: Form of the SST dependent bias adjustment of the V3.0 Aquarius salinity.

In deriving the bias adjustment (Figure 3), it is important to separate the SST dependent biases from rain freshening effects. The first biases are spurious and caused by errors in the Aquarius geophysical model function. The rain freshening biases, however, are caused by stratification and arise because of actual salinity differences in the upper layer near the surface, as described in section 4. The rain filtering and our stratification analysis is an essential part of being able to separate these two biases.

5.3 Evaluation of Bias Adjustment

A significant improvement in the comparison between rain filtered salinity of Aquarius and ARGO after including the SST dependent bias adjustment is evident in both in the global map (Figure 4) and the Hovmoeller plot (Figure 5).

While a comparison of the left and right panels of Figure 4 and Figure 5 might suggest at the first sight that the rain freshening effect has been removed by the bias adjustment, comparing Figure 6 with Figure 2 actually shows that the bias adjustment has the effect of increasing tropical SSS by about 0.17 psu (Table III) while leaving the slope of ΔSSS vs rain rate nearly unchanged. Thus, while the blue (fresh) areas in the tropics in Figure 4 and Figure 5 are in the same location as heavy rain, the monthly average bias is not due to active rain, but has other sources, namely the ones listed in section 5.1.

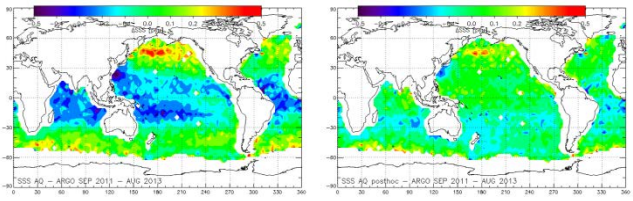

Figure 4: Bias between monthly 150 km means of ocean surface salinity from Aquarius after rain-filtering and ARGO: Left panel: Standard Aquarius V3.0 salinity. Right panel: After including the SST dependent bias adjustment (Figure 3).

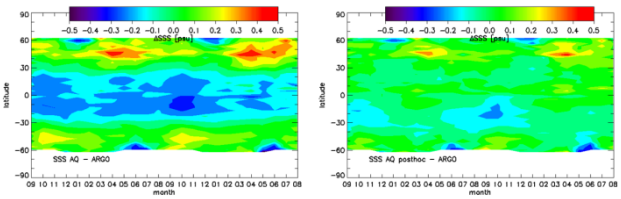

Figure 5: Hovmoeller plot of salinity difference between Aquarius after rain filtered and ARGO. The x-axis denotes month starting with September 2011. The y-axis denotes latitude. Right panel: After including the SST dependent bias adjustment (Figure 3).

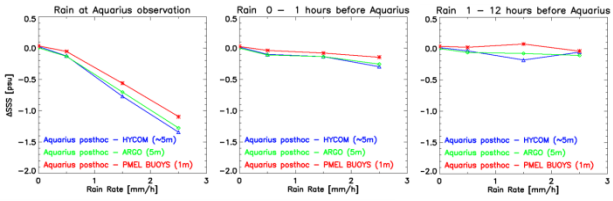

Figure 6: Same as Figure 2 after performing the SST dependent bias adjustment.

6. AQUARIUS V3.0 VERUS CAP SALINITY

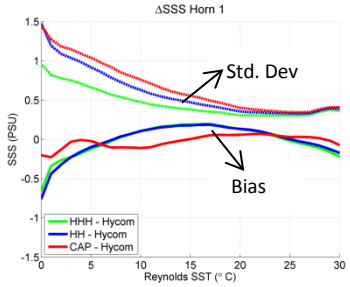

Figure 7: Bias (full lines) and standard deviation (dashed lines) between Aquarius and HYOCM salinity measured at 1.44 sec as function of SST. Green: Standard Aquarius V3.0 algorithm which uses scatterometer (HH) and radiometer (H) wind speeds in the roughness correction. Blue: Using only scatterometer (HH) wind speeds in the roughness correction. Red: CAP algorithm V2.5.1.

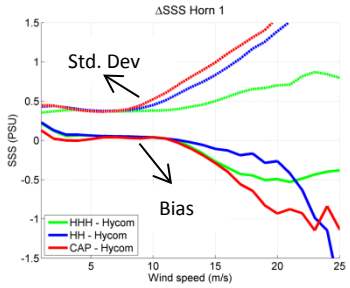

Figure 8: Same as Figure 7 but shown as function of wind speed.

We conclude with a brief comparison between the Aquarius V3.0 salinity and the JPL CAP product [12]. Both products

are retrieved from different algorithms. The differences concern the geophysical model function particular the surface roughness correction, the correction for the reflected galactic radiation and also the antenna pattern correction.

The Aquarius instrument produces salinity measurements at a time resolution of 1.44 seconds, which are recorded in the Level 2 files. When comparing Aquarius SSS with HYCOM or ARGO, the CAP algorithm performs considerably noisier at low SST (Figure 7) and high wind speeds (Figure 8). However, when comparing monthly 100 km averages, where the noise is significantly reduced, the CAP algorithm (Figure 9, red line) has standard deviations that are about 0.02 psu smaller than the Aquarius V3.0 standard product (Figure 9, green line). The reason for that is that the CAP algorithm has tried to reduce the SST dependent biases by tuning the dielectric constant model. This is evident from the full red line in Figure 7. Fine tuning of the dielectric model effectively serves the same purpose as making the SST dependent bias adjustment described in section 5.2, though it is only one of many possible to way to do this. Figure 9 shows that after making the adjustment (black line) the performance of the bias adjusted Aquarius V3.0 salinity is about 0.05 psu smaller than that of the standard Aquarius salinity and about 0.03 psu smaller than that of the CAP product.

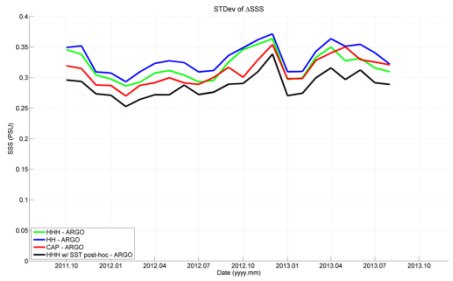

Figure 9: Standard deviation of monthly 100 km averages between Aquarius and ARGO. Green: Standard Aquarius V3.0 algorithm which uses scatterometer (HH) and radiometer (H) wind speeds in the roughness correction. Black: Same as green but adding the SST dependent bias adjustment (section 5.2). Blue: Using only scatterometer (HH) wind speeds in the roughness correction. Red: CAP algorithm V2.5.1.

7. SUMMARY AND CONCLUSIONS

To summarize the main points: Rain rate measurements from the MWR Ku-band radiometer, WindSat, SSMIS and TMI that have been collocated with Aquarius SSS measurements allow an assessment of SSS stratification in the upper ocean layer after rain. In the tropics noticeable rain induced fresh-water lensing can be observed at least up to 1 hour after the rain event.

The standard rain-free Aquarius V3.0 salinity product exhibits salty biases at mid-high latitudes and fresh biases in the tropics and subtropics when compared to ARGO, HYCOM or moored PMEL buoy measurements. Those biases are not related to rain-freshening or stratification but likely caused by a combination of small uncertainties in the geophysical model that is used in the Aquarius salinity retrieval. A post-hoc SST dependent adjustment improves those biases significantly and explains also the observed performance differences between Aquarius V3.0 and the CAP SSS product.

8. REFERENCES

[1] D. LeVine, G. Lagerloef, F. Colomb, S. Yueh, and F. Pellerano, "Aquarius: An instrument to monitor sea surface salinity from space," *IEEE Trans. Geosci. Remote Sens.*, vol. 44, no. 7, pp. 2040 - 2050, 2007.

[2] S. Biswas, L. Jones, D. Rocca, and J.-C. Gallio, "Aquarius/SAC-D Microwave Radiometer (MWR): Instrument description & brightness temperature calibration", doi: 10.1109/IGARSS.2012.6350705, IGARSS 2012.

[3] K. Hilburn and F. Wentz, "Intercalibrated passive microwave rain products from the unified microwave ocean retrieval algorithm (UMORA)", *J. Appl. Meteorol. Climatol.*, vol. 47, pp. 778-794, 2008.

[4] J. Boutin, N. Martin, G. Reverdin, X. Yin, and F. Gillard, "Sea surface freshening inferred from SMOS and ARGO salinity: impact of rain", *Ocean Sci.*, vol. 9, pp. 183 – 192, 2013.

[5] T. Meissner. F. Wentz, D. LeVine, and J. Scott, "Aquarius Salinity Retrieval Algorithm", ATBD, Addendum III, http://podaac.jpl.nasa.gov/SeaSurfaceSalinity/Aquarius.

[6] T. Meissner, F. Wentz, and L. Ricciardulli, "A geophysical model for the emission and scattering of L-band microwave radiation from rough ocean surfaces", submitted to JGR Ocean Special Section Early scientific results from the salinity measuring satellites Aquarius/SAC-D and SMOS, http://www.remss.com/about/profiles/thomas-meissner.

[7] T. Meissner, F. Wentz, L. Ricciardulli, K. Hilburn, and J. Scott, "The Aquarius Salinity Retrieval Algorithm: Recent Progress and Remaining Challenges", Proceedings of MicroRad 2014, http://www.remss.com/about/profiles/thomas-meissner.

[8] W. Tang, S. Yueh, A. Fore, G. Neumann, A. Hayashi, and G. Lagerloef, "The rain effect on Aquarius' L-band sea surface brightness temperature and radar backscatter", *Rem. Sens. Env.*, vol. 137, pp. 147-157, 2013.

[9] T. Meissner and F. Wentz, "The complex dielectric constant of pure and sea water from microwave satellite observations", *IEEE Trans. Geosci. Remote Sens.*, vol.42, no.9, pp. 1836-1849, 2004.

[10] T. Meissner and F. Wentz, " The emissivity of the ocean surface between 6 and 90 GHz over a large range of wind speeds and earth incidence angles", *IEEE Trans. Geosci. Remote Sens.*, vol. 50, no.8, pp, 3004-3026, 2012.

[11] H. Liebe, P. Rosenkranz, and G. Hufford, "Atmospheric 60-GHz oxygen spectrum: New laboratory measurements and line parameters", *J. Quant. Spect. Rad. Transf.*, vol. 48, pp. 629-643, 1992.

[12] S. Yueh, W. Tang, A. Fore, G. Neumann. A. Hayashi, A. Freedman, J. Chaubell, and G. Lagerloef, "L-Band Passive and Active Microwave Geophysical Model Functions of Ocean Surface Winds and Applications to Aquarius Retrieval", *IEEE Trans. Geosci. Remote Sens.*, vol. 51, no. 9, pp. 4619 - 4632, 2013.